Title

Kinetics profiling of gramicidin S synthetase A, a member of nonribosomal peptide synthetases

Funding Source Statement

This work is supported by Human Frontiers Science Program No. RGP0031/2010-C202 award. Financial support from University of Muenster and Princeton University are also gratefully acknowledged.

Authors and Affiliations

Xun Sun[†], Hao Li[†], Jonas Alfermann[‡], Henning D. Mootz[‡], Haw Yang[†]*

†Department of Chemistry, Princeton University, Princeton, NJ 08544, USA

‡Institute of Biochemistry, University of Muenster, 48149 Münster, Germany

*Corresponding author:

Email: hawyang@princeton.edu

Telephone: +1(609)-258-3578

Abbreviations

A: adenylation, C: condensation, CF: cysteine-free, ESI-TOF-MS: electrospray ionization time-of-flight mass- spectrometry, GrsA: gramicidin S synthetase A, HPLC: high-pressure liquid chromatography, NRPS: non-ribosomal peptide synthetase, PCP: peptidyl carrier protein, PP_i: pyrophosphate, TE: thioesterase, WT: wild type.

Abstract

Nonribosomal peptide synthetases (NRPS) incorporate assorted amino acid substrates into complex natural products. The substrate is activated via the formation of a reactive aminoacyl adenylate, and subsequently attached to the protein template via a thioester bond. The reactive nature of such intermediates, however, leads to side reactions that also break down the high-energy anhydride bond. The off-pathway kinetics or their relative weights compared to the on-pathway counterpart remains generally elusive. Here, we introduce multi-platform kinetics profiling to quantify the relative weights of on- and off-pathway reactions. Using the well-defined stoichiometry of thioester formation, we integrate a mass-spectrometry (MS) kinetics assay, a high-performance liquid chromatography (HPLC) assay, and an ATP-pyrophosphate (PP_i) exchange assay to map out a highly efficient on-pathway kinetics profile of the substrate activation and intermediate uploading (>98% relative weight) for the wide-type gramicidin S synthetase A (GrsA) and a 87% rate profile for a cysteine-free GrsA mutant. Our kinetics profiling approach complements the existing enzyme-coupled byproduct-release assays, unraveling new mechanistic insights of substrate activation/channeling in NRPS enzymes.

NRPS produce a myriad of life-saving natural products including potent antibiotics (*e.g.* penicillin) and anti-cancer drugs (*e.g.* bleomycin).[1] These hundreds-of-kilo-Dalton enzymes comprise of distinct domains in a molecular assembly line manner, and each domain is responsible for catalyzing a distinct chemical transformation with a controlled timing to construct natural peptidyl products of remarkable chemical complexity (see Scheme 1A for GrsA as an example).[2] It is precisely because NRPS function in such a modular way, they hold great promise for generating new drug-like molecules through combinatorial biosynthesis.[3, 4] A thorough understanding of the reactivity of individual domains, as well as the assembly line as a whole, is expected to contribute to accelerating new therapeutics discovery.[5]

A minimal NRPS assembly line includes the following four domains: the adenylation domain (A) that activates a cognate amino acid, the peptidyl-carrier protein (PCP) that transfers the covalently attached aminoacyl motif along the assembly line, the condensation domain (C) that catalyzes the peptide bond formation, and the thioesterase domain (TE) that cleaves the product off from the protein template.[6] The activation of various non-proteinogenic amino acid building blocks (>500 precursors[7]) by adenylation domains is achieved via a reactive acyl-adenylate (the adenylation step, *cf.* Scheme 1B).[8] This intermediate then forms a thioester bond with the free thiol group at the 4'-phosphopantetheine (Ppant) in the PCP domain (the thioesterification step, *cf.* Scheme 1B),[9] facilitating the downstream substrate channeling at C, TE and other possible tailoring domains.[10]

To study the enzymatic reactivity along the multi-step NRPS assembly process, a number of kinetic assays have been developed. For example, the ATP-PP_i exchange assay characterizes the adenylation step in A domains,[11] and the radioactive amino acid incorporation in PCP domains characterizes the thioester formation step.[12] These two assays directly measure the on-pathway kinetics. Here the "on" pathway means the reaction pathway (both forward and reverse reactions) that leads to the final product the NRPS is supposed to produce. Assays have also been developed to study the dissociation of on-

pathway byproducts. The enzyme-coupled PP_i assay characterizes the adenylation byproduct release[13] and the enzyme-coupled AMP assay characterizes the thioester formation byproduct release.[14]
On the other hand, enzymes that synthesize reactive acyl-adenylate intermediates including NRPS A domains and t-RNA synthetases, are also capable of catalyzing several "off" pathway reactions (Scheme 1B)—all involve breaking the high-energy anhydride bond (~15 kcal mol^{-1} estimated for carboxyl phosphate[15]). It was shown that, for t-RNA synthetases, the labile acyl-adenylate could react with ATP to form ADP,[16] with phosphate (P_i) to form ADP,[17] with PP_i to form ATP,[11] and with triphosphate (P_3) to form adenosine 5'-tetraphosphate.[18] Rapaport *et al*.[16] and Luo *et al*.[13] demonstrated the existence of the off-pathway side reaction of acyl adenylate with ATP in NRPS. Moreover, the acyl-adenylate could also be removed from the on-pathway reaction either by hydrolysis or by diffusion from the active site so that it becomes unavailable for making the final product. Despite these great advances in understanding the biochemistry of individual NRPS domains, the off-pathway kinetics or their relative weights in the overall reaction remains generally unknown.

Here we put forward a multi-platform approach to address this general problem, and illustrate the kinetics profiling idea with its approach by fully characterizing the kinetics profile of the bi-domain GrsA A-PCP construct. As a model system in the NRPS family, the on-pathway kinetics of GrsA has been extensively studied using the previously mentioned radioactive kinetics assays[11, 12, 19] and the single-turnover analysis[13, 20] whereas the PP_i release kinetics has been reported as well.[13, 20-22] In what follows, we outline our approach to elucidating the hitherto elusive kinetics profiles of on/off pathways of GrsA A-PCP. Its current form only requires facilities and instruments that are common to most institutes, including a radioactive lab, HPLC and MS (Scheme 1B): The ATP-PP_i-exchange to probe the formation of acyl adenylate and its breakdown by PP_i; the MS kinetics assay to visualize the conversion of acyl adenylate to the thioester-bound holo protein, and the UV-HPLC kinetics assay to quantify the

product formation in the remaining side reactions that consume the UV-sensitive acyl adenylate. Due to the μM detection limit in our UV-HPLC for adenosine (Figure S1), mM-substrate and μM-enzyme are mixed to allow μM-product detection over the second to minute timescale; the high reactant concentrations also help to bias the forward reaction in these two-step reversible reactions. We note that the gross AMP formation measured by HPLC could come from 1) the off-pathway hydrolysis of acyl adenylate, and 2) the on-pathway byproduct during thioesterification in holo proteins. To characterize the relative contributions from these two sources, we take advantage of the 1:1 stoichiometry of AMP and acyl-S-protein in the thioester formation: AMP from source 2) could be calculated using the MS-kinetics assay using such stoichiometry and the rest of AMP from source 1) can then be quantified. The MS-based approach is well suited for this purpose; it naturally extends the μM-substrate in the typical radiolabeling kinetics assay to mM-substrate by using unlabeled substrates. In this work, we apply the electrospray ionization time-of-flight MS (ESI-TOF-MS) without digestion or chromatography separation for the MS-kinetics assay of thioesterification in GrsA proteins. This approach expands the application scope of MS analysis from active site mapping[23] or substrate-loading visualization[24, 25] to the direct kinetics monitoring for NRPS proteins.

In this work, we carry out kinetics profiling for a wild-type (WT) A-PCP GrsA construct, and contrast its profile against a previously reported Cys-free (CF) A-PCP construct that has a slightly reduced adenylation activity.[26] In that study, the CF mutant was engineered to enable the selective labeling of the thiol at Ppant, and the solvent-accessibility of the Ppant was investigated with various substrates. In this work, we choose CF as an example for evaluating the potential effect from the site-directed mutagenesis in engineered NRPS constructs. We quantitatively demonstrate that the kinetics changes from all monitored enzymatic reactions in CF—compared to WT—can be promptly reported

via the kinetics profiling. Notably, our results underscore the efficient on-pathway reactivity in WT and CF constructs for both substrate activation (adenylation) and uploading (thioesterification).

Experimental Procedures

Protein Expression, Purification and Modification. The expressions and purification of GrsA proteins were performed similarly as previously reported,[26] with the modification that 10 mM $MgCl_2$ was supplemented during expression. *E. coli* Rosetta (DE3) or BL21-Gold (DE3) was used as the expression strain. An extinction coefficient at 280 nm of 73000 $M^{-1}cm^{-1}$ was used to estimate the protein concentration. The apo-to-holo conversion was performed according to the protocol previously reported.[26] The molecular weight of purified or modified protein was determined by ESI-TOF-MS (Table S1). Unless otherwise noted, characterization experiments were carried out in 50 mM Tris/HCl, 300 mM NaCl and 10 mM $MgCl_2$ (pH 8) under room temperature (25 °C). See Supporting Information for the detailed list of chemical materials used in this work.

HPLC Assay. HPLC experiments were performed in a 1260 HPLC machine (Agilent) with the reversed-phase column was dC18 (4.6 x 100 mm) with 3-μm particle size (Atlantic) and monitored at 254 nm. The running buffer A (more polar) and buffer B (less polar) were prepared according to the work of Luo *et al.*[13]. The elution gradient was set as follows: 0–2 min, 100% A; 2–25 min, 100% A to 33 % B and 0% B to 67 % B; 25–30 min, 33% A and 67% B with the flow rate as 1 mL min^{-1}. The standard chemicals were used to identify the observed peak positions in chromatograms and the concentration calibrations of AMP and L-Phe were performed (Figure S1). 7 μM Apo or holo GrsA was incubated with 1 mM ATP and 1 mM L-Phe at room temperature for 30, 330, 630 and 930 s before the syringe filtering (0.2 μm Nylon) that removed the reactive enzyme from 60–70 μL of solution (Figure S2). Filtrates containing small molecules were kept on ice until being injected for HPLC analysis. HPLC

peak areas were obtained by the OpenLab Intelligent Reporting Software (Agilent, A.01.06.111) with the default integration parameter setting.

ATP-PP_i Exchange Assay. Reactions were initiated by the addition of ATP and Phe (2 mM each) to a mixture of enzyme (300 nM), non-radioactive sodium pyrophosphate (0.2 mM) and 0.15 μCi of ^{32}P-labeled pyrophosphate in a final volume of 100 μL. Experiments were conducted at 28 °C in NRPS-assay buffer (50 mM HEPES, 100 mM NaCl, 1 mM EDTA and 20 mM $MgCl_2$, pH 7). The reaction was allowed to proceed for up to 15 min and then quenched by addition of termination mixture (350 mM perchloric acid, 100 mM cold sodium pyrophosphate, 1.6 % activated charcoal in water). 0-min samples were obtained by mixing protein and substrates directly in the termination mixture, such that no reaction could occur. The quenched samples were mixed vigorously, incubated on ice for 1 min and were centrifuged for 1 min at 13000 rpm (1 °C). Supernatant was removed and charcoal pellets were washed twice by resuspending in 800 μL water and subsequent centrifugation. The pellet was finally resuspended in 500 μL water and added to 2.5 mL of scintillation liquid (Aquasafe 500 plus, Zinsser Analytic GmbH). Scintillation counting was done by averaging counts over 1 minute using a Beckman LS6500 multi purpose scintillation counter. All data points shown are the mean of at least two experiments conducted as triplicates. Experimental data performed with ~1 μM supplemented PP_i was listed in Table S2.

MS Kinetics Assay. Purified protein was desalted using ZipTip (C18) pipette tips prior to the MS analysis. For kinetics measurements, 2 μM enzyme was mixed with 1 mM ATP and 1 mM L-Phe at room temperature, and the sample was desalted at various time point for MS analysis. To desalt the protein sample, one more polar solvent (buffer C, 97% water, 3% acetonitrile and 0.1% formic acid) and one less polar solvent (buffer D, 90% acetonitrile, 10% water and 0.1% formic acid) were used to desalt GrsA proteins. Desalting tips were first cleaned with 20 μL buffer D twice and equilibrated with 20 μL

buffer C twice before use. On average, 2–20 μL 0.3–10 μM protein was loaded into tips and washed in 20 μL of buffer C for at least three times. Desalted protein was eluted out in 9 μL of elution buffer (50% buffer C + 50% buffer D) for the subsequent MS analysis. MS experiments were performed in a 6220 Accurate-Mass Time-of-Flight liquid chromatography/mass spectrometry (Agilent) in the positive ion mode. The running buffer was 50% acetonitrile, 50% water and 0.1% formic acid. The flow rate was 0.125 mL min^{-1}. The acquisition time was 711.9 millisecond/spectra. For ESI-TOF setting, the gas temperature was 325 °C, Vcap was 350 V, nebulizer pressure was set at 30 psig, the fragmentor voltage was 175 V and skimmer voltage was 65 V. The mass window of TOF was set to be the range of 100 to 1600 m/z. Raw mass data were analyzed using the Mass Hunter software (Agilent, Version B. 03.01, Build 3.1.346.0) using a transformation algorithm proposed by Mann *et al*.[27] All multiply charged species were analyzed to obtain the mass of the parent species. The deconvoluted mass window was set to be from 55000 to 80000 Da. Standard compounds of purine ([M+H], 121.050873) and hexakis(1H, 1H, 3H-tetrafluoropropoxy)phosphazine ([M+H], 922.009798) were used to calibrate mass measurements internally.

Thioester Formation ^{3}H Assay. ATP (1 mM), $MgCl_2$ (10 mM) and both cold and ^{3}H-labelled (175:1 ratio) phenylalanine (4 μM) were pre-incubated at 25 °C in a bovine serum albumin (BSA)-coated reaction tube. The reaction was initiated by the addition of the enzymes (a final concentration of 300 nM), TCEP (5 mM) and 50 mM 4-(2-hydroxyethyl)piperazine-1-ethanesulfonic acid (HEPES), 100 mM NaCl, 1 mM ethylenediaminetetraacetic acid (EDTA), 10 mM $MgCl_2$, pH 7 (^{3}H-assay buffer) to yield a final volume of 100 μL per sample. The reaction mixture was incubated at 25 °C and samples of 100 μL were taken at specified time points. The reaction was quenched by the addition of 800 μL of ice-cold trichloroacetic acid (TCA, 10%) and 15 μL BSA (25 mg mL^{-1}) to the reaction mixture. The protein fraction was precipitated by incubation on ice for 30 min and subsequently centrifuged at 13000 rpm for

30 min (1 °C). Pellets were washed with 800 µL TCA (10%) twice to remove unbound substrates and re-dissolved in 150 µL formic acid (98%). The solution was thoroughly mixed with 2.5 mL liquid scintillation fluid and radioactivity of the ^{3}H-labelled protein was determined by liquid scintillation counting, averaging over 5 minutes using a Beckman LS6500 multi purpose scintillation.

Profiling Data Analysis. The non-linear kinetics of AMP formation in holo GrsA was described by the following equation:

$$\left[\mathrm{AMP}(t)\right]_{\mathrm{holo}} = \left[\mathrm{Enz}\right]\left(A - B\exp\left(k_{\mathrm{obs}}^{\mathrm{ESI}}t\right)\right) + \left[\mathrm{Enz}\right]k_{\mathrm{holo}}^{\mathrm{hydro}}t \quad (1)$$

where the single-exponential component in first term is from ESI-TOF-MS experiments (Figure S15), $k_{\mathrm{holo}}^{\mathrm{hydro}}$ is the time constant for Phe-AMP hydrolysis in holo enzymes and $\left[\mathrm{Enz}\right]$ is the enzyme concentration. This is the key equation that integrates the HPLC and ESI-TOF-MS measurements. The remaining product formation kinetics was found to be linear within the first 15 min of the reaction; therefore these kinetics data were fit to a zero-order kinetic model:

$$\left[\mathrm{product}(t)\right] = \left[\mathrm{Enz}\right]kt + C \quad (2)$$

where k is the rate constant for corresponding reaction and C is a fitting parameter. We then normalized the linear slope ($\left[\mathrm{Enz}\right]k$, µM s^{-1}) of product formations using the GrsA protein concentration to obtain rate constants (s^{-1}) in a similar way as previously reported.[28] Since all enzymatic reactions involve the Phe-AMP intermediate, the overall observed rate of Phe-AMP ($k_{\mathrm{apo/holo}}^{\mathrm{PheAMP}}$) can be expressed by:

$$k_{\mathrm{apo/holo}}^{\mathrm{PheAMP}} = k_{\mathrm{apo/holo}}^{\mathrm{hydro}} + \frac{1}{2}k_{\mathrm{apo/holo}}^{\mathrm{ADP}} + k_{\mathrm{obs}}^{\mathrm{ESI}} + k_{\mathrm{apo/holo}}^{\mathrm{loss}} + k_{\mathrm{apo/holo}}^{\mathrm{PPi}} \quad (3)$$

where $k_{\mathrm{apo/holo}}^{\mathrm{hydro}}$ is the Phe-AMP hydrolysis rate, $k_{\mathrm{apo/holo}}^{\mathrm{ADP}}$ is the rate of ADP side reaction, $k_{\mathrm{obs}}^{\mathrm{ESI}}$ is the Ppant modification rate from ESI-TOF-MS (0 for apo protein), $k_{\mathrm{apo/holo}}^{\mathrm{loss}}$ is the net release rate of diffused Phe-AMP and $k_{\mathrm{apo/holo}}^{\mathrm{PPi}}$ is the rate for the adenylation reaction. The fact of 2 comes from the stoichiometry of

ATP in this ADP side reaction (Scheme 1B(2)). See Supporting Information for more detailed analysis and supplementary experimental methods. Unless otherwise noted, experiments were independently performed three times and results were reported as mean ± one standard deviation, analyzed using MATLAB (Mathworks, R2013a).

Results and Discussions

Kinetics Profiling of Apo Proteins. We first established an HPLC protocol to monitor at 254 nm UV-sensitive small molecules (AMP, ADP and Phe) to quantify their concentrations on the range of μM (Figures S1–S2). Under our experimental condition, the Phe-AMP remained stable (Figure S3A). We then measured the kinetics of apo WT/CF (Figure 1A) using HPLC/ATP-PP_i-exchange. Linear kinetics of AMP, ADP and Phe-AMP were clearly shown by HPLC (Figures 1B–1D) and such formation of products were assumed to be dependent on the enzymatic reaction since the ATP plus L-Phe was stable at room temperature for a timespan longer than the HPLC runtime without enzyme (Figure S3B) and that the omission of L-Phe led to no newly formed of AMP or ADP or Phe-AMP given the μM detection limit of our HPLC for adenosine-bearing motif (Figure S4). Due to the absence of the on-pathway byproduct AMP from the thioesterification in the apo enzyme without the background Ppant modification during expression (Figure S5), all AMP in this experiment is assumed to be from the off-pathway hydrolysis of Phe-AMP (Scheme 1B(1)). ADP presumably is from the off-pathway side reaction of Phe-AMP and ATP (Scheme 1B(2)), whereas the observed free Phe-AMP probably dissociates from its binding pocket within the A domain (another off-pathway in Scheme 1B(3)). For the on-pathway adenylation reaction, we observed a Henri-Michaelis-Menten–type kinetics depending on supplemented PP_i concentration (Figure 2), suggesting that the sum of forward and reverse adenylation is proportional to the supplemented PP_i concentration when the latter is far smaller than the Michaelis-Menten constant. We then estimated the PP_i concentration in the HPLC assay and used it to estimate the

rate of the adenylation (see details in Supporting Information). As expected, the rate of the on-pathway adenylation reaction in the apo WT contributes ~80% of the overall rate. Such on-pathway kinetics weight is reduced to ~55% in apo CF (Table 1; see Supporting Information for kinetics equations and quantifications).

Verification of the MS assay. Since the MS-kinetics assay was needed to quantify the kinetics of holo WT and holo CF, we first proceeded to verify the accuracy of our ESI-TOF-MS assay for the 70-kDa GrsA constructs and obtained correct molecular weights compared to calculated ones for both apo and holo protein, with or without aminoacyl modification (Table S1, Figure S5–S6). We also confirmed the stability of Phe-S-protein (M+147) under our experimental conditions (Figure S7). As expected, such aminoacylation was ATP-dependent in holo constructs and completed within 10 min at room temperature for both holo proteins (Figure S6). By contrast, incubating apo WT/CF with both substrates for 1 hr did not result in the Phe-adduct peak, consistent with the "swinging-arm" model[29, 30] that the Ppant attached to the arguably highly mobile holo PCP is rapidly aminoacylated in our MS kinetics assay (Figure S8). Interestingly, we observed the autoaminoacylations with multiple covalent L-phenylalaminoacyl adduct (M+147x, x = 1,2 …) in the incubation over days, analogous to what has been observed for several tRNA synthetases.[31, 32]

Having confirmed the measurement accuracy and the stability of acyl-S-protein under our experimental conditions, we set out to validate our MS-based kinetics method by comparing it to the standard radiolabeling assay. We first manually desalted holo CF from ATP/L-Phe at various time points within a 15-min reaction time window. A series of time-dependent mass spectra clearly showed the conversion from free holo CF to Phe-loaded holo CF (Figure 3A). As demonstrated by the pioneering work of the Kelleher group, an accuracy of ~5% error in estimating relative protein concentrations could be achieved for (un)modified full-length GrsA ionized via ESI.[24] We normalized

the percentages of L-Phe–loaded protein using the deconvoluted mass peak heights.[27] We then obtained the thioester formation kinetics from a first-order kinetics model ($(4.7\pm0.9)\times10^{-3}$ s^{-1}, *c.f.* Figure 3B) that was in quantitative agreement with the standard L-[^{3}H]-Phe assay under the same experimental condition ($(4.2\pm0.1)\times10^{-3}$ s^{-1}, *cf.* Figure S9). In contrast, the thioester formation of holo WT was complete within 6 s at room temperature (Figure S6) in agreement with a previous report on full-length GrsA using the radioactive assay.[19] A ~10-fold increase in L-Phe binding constant (K_d) (Figure S10) and the less compact global conformation (Figures S11–S12) may account for the observed slower rate for the inter-domain thioester formation in holo CF. Nevertheless, these results allowed a lower bound for the thioester formation kinetics in holo WT with saturated substrates (Figure S13).

Kinetics Profiling of holo Proteins. After establishing the suitability and accuracy of HPLC and MS kinetics experiments, we next performed the full kinetics profiling for holo WT and CF proteins. Within 15-min incubation time at room temperature, HPLC-analysis clearly demonstrated the linear kinetics of ADP and Phe-AMP formation for holo CF (Figures 4B–4C and S14). In contrast, a non-linear AMP formation kinetics was observed (Figure 4A). This result was expected since the sum of the first-order thioester formation (Figure S15) and the zero-order hydrolysis (with respect to the enzyme) could give rise to such non-linear AMP formation. Put together, the kinetics profile of holo CF showed a ~82% weight for thioester-formation kinetics and a ~87% weight for both adenylation and thioesterification (Table 1). In the case of holo WT, the lower bound of the relative weight was of 91% for thioester formation and 98% for both adenylation and thioester formation. Interestingly, the non-linear kinetics feature in holo CF AMP formation was clearly absent in holo WT (Figure 4A); this is because the first order thioester formation was completed before the first HPLC time point (30 s) and only the linear Phe-AMP hydrolysis was monitored post thioesterification. Furthermore, due to the rapid formation of one equivalent of AMP (~7 μM), the AMP concentration in holo WT at the first time point

(30 s) was expected to be much more than that of its apo or CF counterpart (~2–3 μM). Indeed, it was shown via the HPLC analysis of holo WT that it was the case (Figure 4A). Similar to apo CF/WT, linear kinetics of ADP and Phe-AMP were observed for holo WT.

Collectively, these kinetics-profiling experiments clearly indicated that, with excess substrates, holo WT GrsA keeps consuming acyl-adenylate intermediates but at a slower rate after the completed Ppant aminoacylation. Such kinetics, manifested by a rapid initial burst followed by a slower increase, has also been observed in homologous enzymes.[14, 28, 33] Furthermore, our profiling may provide a kinetic basis for the previous reports where a second equivalent of the cognate amino acid and ATP can be consumed before the Ppant is discharged again:[33, 34] Although the tight binding between the second equivalent acyl adenylate and the NRPS A domain as well as the loaded Ppant may inhibit the next-round on-pathway reaction, all the off-pathway reactions (Scheme 1B(1)–(3)) could still occur post thioesterification. These concurrently occurring off-pathway reactions consume the second equivalent acyl adenylate intermediate at a much slower summed rate (at least 53-fold reduced compared to thioesterification), as first reported here, ensuring the observed 2× stoichiometry in the substrate consumption. Conceivably, the breakdown of the enzyme-intermediate complex post the thioesterification to recover the free enzyme capable of reinitiating another round of catalysis is a slow step, if not the rate-limiting one. Along a similar vein, the profiled WT holo kinetics is also consistent with the finding that only one equivalent of AMP can be measured[35] due to the negligible off-pathway acyl adenylate hydrolysis rate compared to the on-pathway thioester formation rate (Table 1).

Mechanistically, the observed highly efficient on-pathway kinetics profile of thioester formation in the GrsA A-PCP bi-domain construct can be attributed to the higher nucleophilicity of the sulfur at Ppant as compared to the oxygen in solvents or competing substrates; it also suggests that the labile Phe-AMP is well protected while waiting to be “channeled” by the mobile Ppant in PCP, presumably in

certain catalytic conformation(s). Kinetic models incorporating two alternating catalytic conformations have been proposed;[14, 28, 36] yet the detailed interplays between conformation and chemistry in NRPS warrant further investigations.

Conclusion In this work, we have demonstrated an integrated multi-platform enzymatic kinetics profiling approach to quantify chemical reactions associated with the reactive acyl-adenylate in NRPS A-PCP domains. We showcase one of its immediate applications by revealing highly efficient adenylation-thioesterification in the WT GrsA A-PCP construct. Local perturbations, as illustrated here by the amino acid substitutions in the CF mutant protein, can lead to deviations from this highly optimized pathway. This point should be considered in biocombinatorial approaches using engineered NRPS in future. Technically, such kinetics profiling well complements other established enzymatic assays, such as the enzyme-coupled assays for the PP_i and AMP release, enabling a comprehensive kinetic perspective for NRPS systems. It is noteworthy to point out that the kinetics profiling approach as reported here could be expanded to measure fast kinetics processes when coupled with a rapid-quenching apparatus. Indeed, based on the success of the present work, one could envision other ways of profiling the kinetics of a molecular assembly line so long as the approach conform to the following attributes: (a) The method must be able to simultaneously follow the time course of many—ideally all—reactants, intermediates, and products. (b) If more than one method is used in profiling, data from different sources must be quantitatively integrated. (c) Perform cross-validation for results from different sources whenever possible. We anticipate that the kinetics profiling idea would offer valuable readout when investigating the molecular basis for such highly efficient on-pathway kinetics in NRPS A-PCP domains or other homologous adenylation protein families.

Acknowledgements

We wish to thank J. Eng for the technical assistance in ESI-TOF-MS experiments, J. Diecker for the technical assistance in radioactive assays and D. Fiedler for the use of HPLC.

Supporting Information

Supplementary experimental methods with 2 supplementary tables and 16 supplementary figures are included in Supporting Information. This material is available free of charge via the Internet at http://pubs.acs.org.

References

(1) Felnagle, E. A., Jackson, E. E., Chan, Y. A., Podevels, A. M., Berti, A. D., McMahon, M. D., and Thomas, M. G. (2008) Nonribosomal peptide synthetases involved in the production of medically relevant natural products, *Mol. Pharm. 5*, 191–211.

(2) Fischbach, M. A., and Walsh, C. T. (2006) Assembly-line enzymology for polyketide and nonribosomal peptide antibiotics: Logic, machinery, and mechanisms, *Chem. Rev. 106*, 3468–3496.

(3) Mootz, H. D., Schwarzer, D., and Marahiel, M. A. (2000) Construction of hybrid peptide synthetases by module and domain fusions, *Proc. Natl. Acad. Sci. U.S.A. 97*, 5848–5853.

(4) Nguyen, K. T., Ritz, D., Gu, J. Q., Alexander, D., Chu, M., Miao, V., Brian, P., and Baltz, R. H. (2006) Combinatorial biosynthesis of novel antibiotics related to daptomycin, *Proc. Natl. Acad. Sci. U.S.A. 103*, 17462–17467.

(5) Cane, D. E., Walsh, C. T., and Khosla, C. (1998) Harnessing the biosynthetic code: combinations, permutations, and mutations, *Science 282*, 63–68.

(6) Marahiel, M. A., Stachelhaus, T., and Mootz, H. D. (1997) Modular peptide synthetases involved in nonribosomal peptide synthesis, *Chem. Rev. 97*, 2651–2674.

(7) Caboche, S., Leclère, V., Pupin, M., Kucherov, G., and Jacques, P. (2010) Diversity of monomers in nonribosomal peptides: Towards the prediction of origin and biological activity, *J. Bacteriol. 192*, 5143–5150.

(8) Berg, P. (1956) Acyl adenylates: An enzymatic mechanism of acetate activation, *J. Biol. Chem. 222*, 991–1013.

(9) Stein, T., Vater, J., Kruft, V., Otto, A., WittmannLiebold, B., Franke, P., Panico, M., McDowell, R., and Morris, H. R. (1996) The multiple carrier model of nonribosomal peptide biosynthesis at modular multienzymatic templates, *J. Biol. Chem. 271*, 15428–15435.

(10) Wu, N., Tsuji, S. Y., Cane, D. E., and Khosla, C. (2001) Assessing the balance between protein-protein interactions and enzyme-substrate interactions in the channeling of intermediates between polyketide synthase modules, *J. Am. Chem. Soc. 123*, 6465–6474.

(11) Gevers, W., Kleinkauf, H., and Lipmann, F. (1968) The activation of amino acids for biosynthesis of gramicidin S, *Proc. Natl. Acad. Sci. U.S.A. 60*, 269–276.

(12) Stachelhaus, T., and Marahiel, M. A. (1995) Modular structure of peptide synthetases revealed by dissection of the multifunctional enzyme GrsA, *J. Biol. Chem. 270*, 6163–6169.

(13) Luo, L., and Walsh, C. T. (2001) Kinetic analysis of three activated phenylalanyl intermediates generated by the initiation module PheATE of gramicidin S synthetase, *Biochemistry 40*, 5329–5337.

(14) Wu, R., Cao, J., Lu, X., Reger, A. S., Gulick, A. M., and Dunaway-Mariano, D. (2008) Mechanism of 4-chlorobenzoate:coenzyme a ligase catalysis, *Biochemistry 47*, 8026–8039.

(15) Lipmann, F. (1944) Enzymatic synthesis of acetyl phosphate, *J. Biol. Chem. 155*, 55–70.

(16) Rapaport, E., Remy, P., Kleinkauf, H., Vater, J., and Zamecnik, P. C. (1987) Aminoacyl-tRNA synthetases catalyze AMP–>ADP–>ATP exchange reactions, indicating labile covalent enzyme-amino-acid intermediates, *Proc. Natl. Acad. Sci. U.S.A. 84*, 7891–7895.

(17) Guédon, G., Ebel, J. P., and Remy, P. (1987) Yeast phenylalanyl-tRNA synthetase: Evidence for the formation of ADP by phosphorolysis of enzyme-bound aminoacyladenylate, *Biochimie 69*, 1175–1181.

(18) Güranowski, A., Sillero, M. A. G., and Sillero, A. (1994) Adenosine 5'-tetraphosphate and adenosine 5'-pentaphosphate are synthesized by yeast acetyl-coenzyme-A synthetase, *J. Bacteriol. 176*, 2986–2990.

(19) Stachelhaus, T., Mootz, H. D., Bergendahl, V., and Marahiel, M. A. (1998) Peptide bond formation in nonribosomal peptide biosynthesis—Catalytic role of the condensation domain, *J. Biol. Chem. 273*, 22773–22781.
(20) Luo, L., Burkart, M. D., Stachelhaus, T., and Walsh, C. T. (2001) Substrate recognition and selection by the initiation module PheATE of gramicidin S synthetase, *J. Am. Chem. Soc. 123*, 11208–11218.
(21) Chen, C. Y., Georgiev, I., Anderson, A. C., and Donald, B. R. (2009) Computational structure-based redesign of enzyme activity, *Proc. Natl. Acad. Sci. U.S.A. 106*, 3764–3769.
(22) Stevens, B. W., Lilien, R. H., Georgiev, I., Donald, B. R., and Anderson, A. C. (2006) Redesigning the PheA domain of gramicidin synthetase leads to a new understanding of the enzyme's mechanism and selectivity, *Biochemistry 45*, 15495–15504.
(23) Stein, T., Vater, J., Kruft, V., Wittmannliebold, B., Franke, P., Panico, M., Mcdowell, R. M., and Morris, H. R. (1994) Detection of 4'-phosphopantetheine at the thioester binding-site for L-valine of gramicidins synthetase-2, *FEBS Lett. 340*, 39–44.
(24) Miller, L. M., Mazur, M. T., McLoughlin, S. M., and Kelleher, N. L. (2005) Parallel interrogation of covalent intermediates in the biosynthesis of gramicidin S using high-resolution mass spectrometry, *Protein Sci. 14*, 2702–2712.
(25) Hicks, L. M., Mazur, M., Miller, L. M., Dorrestein, P. C., Schnarr, N. A., Khosla, C., and Kelleher, N. L. (2006) Investigating nonribosomal peptide and polyketide biosynthesis by direct detection of intermediates on > 70 kDa polypeptides by using Fourier-transform mass spectrometry, *ChemBioChem 7*, 904–907.
(26) Zettler, J., and Mootz, H. D. (2010) Biochemical evidence for conformational changes in the cross-talk between adenylation and peptidyl-carrier protein domains of nonribosomal peptide synthetases, *FEBS J. 277*, 1159–1171.
(27) Mann, M., Meng, C. K., and Fenn, J. B. (1989) Interpreting mass-spectra of multiply charged ions, *Anal. Chem. 61*, 1702–1708.
(28) Tian, Y., Suk, D. H., Cai, F., Crich, D., and Mesecar, A. D. (2008) *Bacillus anthracis o*-succinylbenzoyl-CoA synthetase: Reaction kinetics and a novel inhibitor mimicking its reaction intermediate, *Biochemistry 47*, 12434–12447.
(29) Perham, R. N. (2000) Swinging arms and swinging domains in multifunctional enzymes: Catalytic machines for multistep reactions, *Annu. Rev. Biochem. 69*, 961–1004.
(30) Tanovic, A., Samel, S. A., Essen, L. O., and Marahiel, M. A. (2008) Crystal structure of the termination module of a nonribosomal peptide synthetase, *Science 321*, 659–663.
(31) Kern, D., Lorber, B., Boulanger, Y., and Giege, R. (1985) A Peculiar property of aspartyl-transfer RNA synthetase from bakers' yeast: Chemical modification of the protein by the enzymatically synthesized aminoacyl adenylate, *Biochemistry 24*, 1321–1332.
(32) Hountondji, C., Beauvallet, C., Pernollet, J. C., and Blanquet, S. (2000) Enzyme-induced covalent modification of methionyl-tRNA synthetase from *Bacillus stearothermophilus* by methionyl-adenylate: Identification of the labeled amino acid residues by matrix-assisted laser desorption-ionization mass spectrometry, *J. Protein. Chem. 19*, 563–568.
(33) Kittelberger, R., Pavela-Vrancic, M., and von Döhren, H. (1999) Active site titration of gramicidin S synthetase 2: Evidence for misactivation and editing in non-ribosomal peptide biosynthesis, *FEBS Lett. 461*, 145–148.
(34) Kallow, W., von Döhren, H., and Kleinkauf, H. (1998) Penicillin biosynthesis: Energy requirement for tripeptide precursor formation by delta-(L-alpha-aminoadipyl)-L-cysteinyl-D-valine synthetase from Acremonium chrysogenum, *Biochemistry 37*, 5947–5952.

(35) Roskoski, R., Jr., Gevers, W., Kleinkauf, H., and Lipmann, F. (1970) Tyrocidine biosynthesis by three complementary fractions from Bacillus brevis (ATCC 8185), *Biochemistry 9*, 4839–4845.
(36) Gulick, A. M. (2009) Conformational dynamics in the acyl-CoA synthetases, adenylation domains of non-ribosomal peptide synthetases, and firefly luciferase, *ACS Chem. Biol. 4*, 811–827.

Tables

Table 1. Kinetics profiling of apo/holo WT/CF GrsA A-PCP constructs with saturated ATP/L-Phe

Rate (s^{-1})	AMP-forming hydrolysis	ADP-forming reaction	Phe-AMP diffusion	Adenylation reaction	Thioesterification reaction	Sum of rates
Apo WT	$(7.2\pm0.1)\times10^{-4}$	$(3.9\pm1.3)\times10^{-4}$	$(3.6\pm0.1)\times10^{-4}$	$(6.2\pm0.8)\times10^{-3}$	0	$(7.7\pm0.8)\times10^{-3}$
Apo CF	$(1.2\pm0.1)\times10^{-3}$	$(6.2\pm0.6)\times10^{-4}$	$(2.3\pm0.2)\times10^{-4}$	$(2.6\pm0.2)\times10^{-3}$	0	$(4.7\pm0.2)\times10^{-3}$
Holo WT	$(6.0\pm0.1)\times10^{-4}$	$(3.1\pm0.3)\times10^{-4}$	$(1.8\pm0.4)\times10^{-4}$	$(4.9\pm0.4)\times10^{-3}$	$> 5.8\times10^{-2}$	$>6.4\times10^{-2}$
Holo CF	$(5.9\pm2.2)\times10^{-4}$	$(4.1\pm2.1)\times10^{-4}$	$(8.7\pm2.3)\times10^{-5}$	$(0.6\pm0.1)\times10^{-3}$	$(9.0\pm1.4)\times10^{-3}$	$(1.1\pm0.1)\times10^{-2}$

Schemes

Scheme 1. (A) The gene cluster for the biosynthesis of gramicidin S. E: epimerization domain (see text for other acronyms). (B) On-/off-pathways of the reactive phenylalanyl adenylate intermediate for the L-Phe activation.

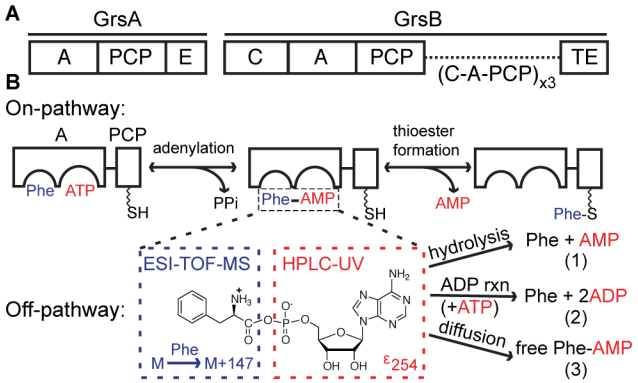

Figure Legends

Figure 1. HPLC analysis for the side reactions in apo WT/CF GrsA. (A) Representative time-dependent HPLC traces of apo WT with ATP + L-Phe. The absorbance is shown on a log scale. b–d) Linear kinetics of AMP (B), ADP (C) and diffused Phe-AMP formation (D) in apo WT (dash fitting line) and in apo CF (solid fitting line). Error bars represent one standard deviation from three repeats.

Figure 2. The rate of adenylation depends on the PP_i concentration for apo WT. A Henri-Michaelis-Menten–type equation is used to fit the adenylation rate data at different PP_i concentrations. Error bars represent one standard deviation from at least three repeats.

Figure 3. ESI-TOF-MS kinetic assay for holo CF with μM-Phe. (A) Representative mass traces showing the conversion from CF holo to Phe-S-protein. (B) Kinetics of the thioester formation reaction. Error bars are one standard deviation from three repeats.

Figure 4 HPLC analysis of holo WT/CF GrsA. Kinetics of AMP (A), ADP (B) and Phe-AMP (C) in holo WT (dash fitting line) and in holo CF (solid fitting line). Error bars represent one standard deviation from three repeats.

Figure

Figure 1

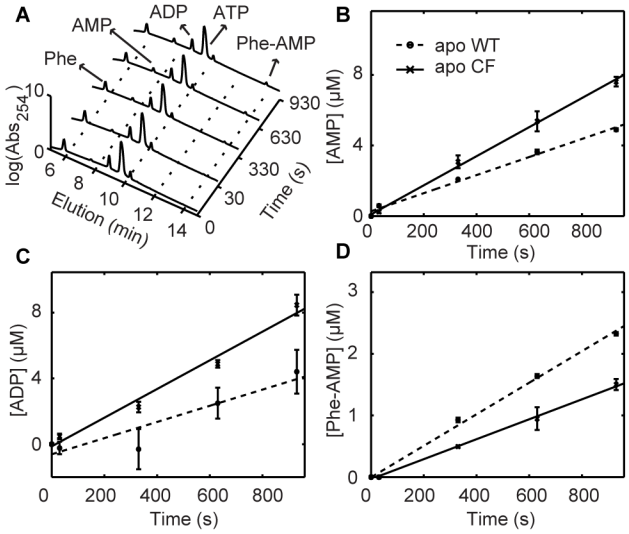

Figure 2

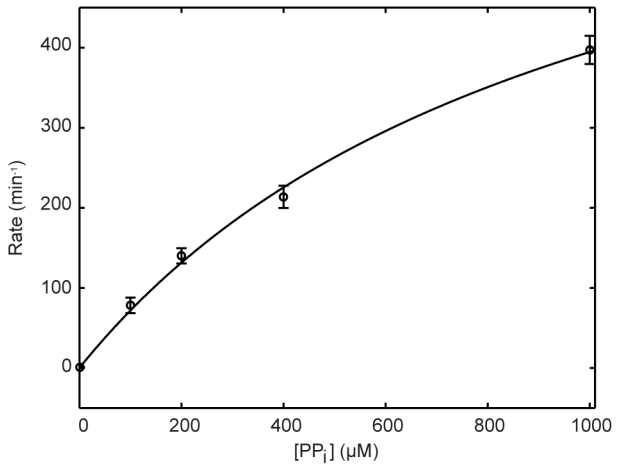

Figure 3

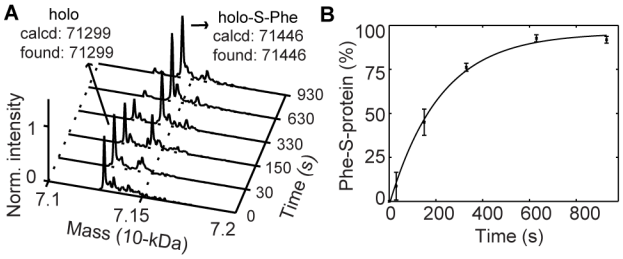
A
holo
calcd: 71299
found: 71299
holo-S-Phe
calcd: 71446
found: 71446
930
630
330
150
30
0
Time (s)
Norm. intensity
1
0
7.1
7.15
7.2
Mass (10-kDa)
B
Phe-S-protein (%)
100
75
50
25
0
0
200
400
600
800
Time (s)

Figure 4

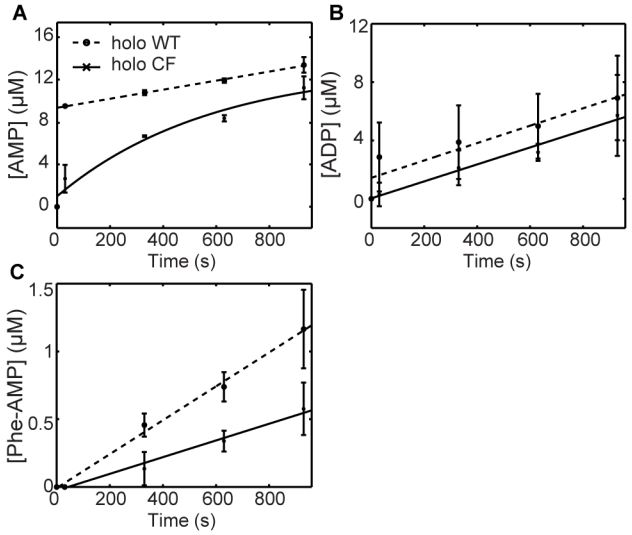

Graphic of the Table of Contents